Analysis of ICESat data using Kalman filter and kriging to study height changes in East Antarctica

A. T. Nguyen and T. A. Herring

Department of Earth, Atmospheric and Planetary Sciences, Massachusetts Institute of Technology, Cambridge, Massachusetts, USA

Received 1 August 2005; revised 12 October 2005; accepted 25 October 2005; published 24 November 2005.

[1] We analyze ICESat derived heights collected between Feb.03–Nov.04 using a kriging/Kalman filtering approach to investigate height changes in East Antarctica. The model's parameters are height change to an *a priori* static digital height model, seasonal signal expressed as an amplitude B and phase θ, and height-change rate *dh/dt* for each (100 km)^2 block. From the Kalman filter results, *dh/dt* has a mean of -0.06 m/yr in the flat interior of East Antarctica. Spatially correlated pointing errors in the current data releases give uncertainties in the range 0.06 m/yr, making height change detection unreliable at this time. Our test shows that when using all available data with pointing knowledge equivalent to that of Laser 2a, height change detection with an accuracy level 0.02 m/yr can be achieved over flat terrains in East Antarctica. **Citation:** Nguyen, A. T., and T. A. Herring (2005), Analysis of ICESat data using Kalman filter and kriging to study height changes in East Antarctica, *Geophys. Res. Lett.*, *32*, L23S03, doi:10.1029/2005GL024272.

1. Introduction

[2] In 2003, NASA launched the Ice Cloud and land Elevation Satellite (ICESat) with the Geoscience Laser Altimeter System (GLAS) onboard. One of ICESat scientific objectives is to study changes in the ice sheet surface heights to improve our understanding of the ice sheets mass balance and their contributions to sea-level changes [*Zwally et al.*, 2002]. With a global coverage of ±86° latitude at along-track spacing of ~172 m, GLAS is the first laser altimeter to offer us a high precision data set, with sufficient spatial and temporal coverage to address the mass balance issue in Antarctica [*Zwally et al.*, 2002].

[3] Over the Antarctic ice sheet, height change (*dh/dt*) detections using spaceborne altimetry measurements are typically calculated by averaging height differences at cross-over locations over large areas and long periods of time [*Zwally et al.*, 1989]. The main advantage of this method is that measurements are interpolated over short distances (less than the along-track spacing) to the same locations, and that any change likely reflects real *dh/dt*. Errors are typically large per cross-over, but decrease when averaged over large areas and time as the square root of the number of cross-overs used [*Zwally et al.*, 1989]. However this approach only uses <10% of the available data. In addition, implementation of cross-over analysis often bins data as a function of time, adding an additional assumption that during the binning interval, the heights remain constant. In this paper we develop an alternate approach to the spatio-temporal *dh/dt* detection problem to assess whether height change detection with accuracy of 2 cm/yr over (100 km)^2 areas is possible. We present preliminary results of processed ICESat heights over East Antarctica using a combined kriging/Kalman filtering technique to evaluate the technique's capability and current data releases quality.

2. ICESat Data

[4] We use estimates of geodetic height above the reference ellipsoid from the most recent releases of GLA06 Global Elevation Data Product and energy and gain from GLA01 Global Altimetry Data Product and GLA05 Global Waveform-based Range Corrections Data (Table 1). Laser 1, 2b–2c are excluded from our analysis because of their current large pointing errors (Table 1). Only shots with laser pointing angles within ±0.03° of the spacecraft nominal pointing of 0.33° are used. We apply the saturation correction to all shots with gain = 13 using the formula given by *Fricker et al.* [2005] (for releases earlier than 22, we multiply the received energy by a factor 1.21, and for releases earlier than 19, we correct for the gain record mis-registration (D. Yi, personal communication, 2005)). We also exclude all shots with gain more than 100 (a pseudo cloud-filter). For shots with gain between 14 and 100, we use only those shots with energy <13.1fJ. The amount of data eliminated by these two editing criteria varies during laser operations and between lasers, <4% of Laser 2a and ~4% for Laser 3a.

3. Method

[5] The model used in the filter relates a parametric description of the ice sheet surface and its time variation to individual laser height measurements. The filter is formulated in regions in which it is assumed that the seasonal signal and height rate of changes are the same across the region. An *a priori* digital height model (DEM) at resolution 5-km is calculated using averaging. For the study presented here, within each (100 km)^2 block containing N number of 5-km DEM elements, we interpolated the DEM to locations of the individual laser spots using kriging. A detailed description of kriging is given by *Olea* [1999]. The Kalman filter state vector $\mathbf{x}$ is given by

$$\mathbf{x} = \left[\delta_{dem1} \ \cdots \ \delta_{demN} \ B_1 \ B_2 \ \Delta_{DEM} \ \frac{dh}{dt}\right]^T \qquad (1)$$

where Δ_{DEM} and δ_{dem_i} are the adjustments in overall (100 km)^2 block height and individual 5-km element height,

0094-8276/05/2005GL024272$05.00

Table 1. ICESat Derived Height Biases for Various Laser Operation Periods (Laser Ops) and Data Releases (REL)

Laser Ops	REL	Start Date (M-D-Y)	End Date (M-D-Y)	Global Pointing Bias,[a] (arcsec)	"Vertical Bias in centimeters Due to Pointing Bias for Surface Slopes:[a]" 0.1°	0.3°	0.5°
1	18	02/20/03	03/29/03	5.83	2.9	8.9	14.8
2a	21	09/25/03	11/18/03	0.94	0.5	1.5	2.5
2b	16	02/17/04	03/21/04	8.07	4.1	12.3	20.5
2c	17	05/18/04	06/21/04	23.99	12.2	36.5	60.9
3a	22	10/04/04	11/08/04	2.21	1.1	3.4	5.6

[a]S. B. Luthcke et al. (personal communication, 2005).

respectively, *dh/dt* is the height-change rate of the block, and the two parameters B_1 and B_2 are the cosine and sine components of the seasonal signal. As a function of amplitude and phase, we have

$$h_{seasonal} = B \cdot \cos\left(2\pi \frac{\delta t - \theta}{365}\right) \qquad (2)$$

with $B_1 = B\cos\theta$ and $B_2 = B\sin\theta$, where B and θ are the amplitude and phase respectively. δt is the time referenced to Jan 01, 2003. The average term Δ_{DEM} is used to avoid possible biases from the zero mean error assumption. The observation equation used is

$$\mathbf{z} = \mathbf{A} \cdot \mathbf{x} + \mathbf{v} \qquad (3)$$

$$\mathbf{A} = \left[w_1 \cdots w_N \; \cos\left(2\pi \frac{\delta t}{365}\right) \; \sin\left(2\pi \frac{\delta t}{365}\right) \; 1 \; 0 \right] \qquad (4)$$

where **z** is the observed minus the interpolated height, **A** the Jacobian matrix, and **v** the data noise. The elements in **A** are the kriging weights w_i which are computed from the statistics of the residuals between surface heights and the DEM, the seasonal cosine and sine terms, and 1 and 0 for Δ_{DEM} and *dh/dt*. We used a standard Kalman filter formulation with process noise set to zero to add data to the filter and update the state vector and its covariance matrix [*Brown and Hwang*, 1997]. *A priori* uncertainties are assumed 400 m^2 for δ_{dem_i}, Δ_{DEM}, B_1, B_2 and 400 m^2/yr^2 for *dh/dt*. These values are loosely constrained relative to the data. We assumed data noise $\mathbf{v} \sim N(0, \mathbf{1}\ \mathrm{m}^2)$. Figure 1 shows the studied region (259 blocks) and one (100 km)^2 DEM block.

4. Results and Discussion

[6] Figure 2 shows the Kalman filter results of the adjustment and uncertainty in *dh/dt* using Laser 2a and 3a. With only two data periods, we exclude the seasonal terms from our analysis due to lack of data. We divide our studied area into 2 regions based on surface slope. The first region, we refer to as LB, includes the steepest part of the Lambert Glacier/Amery Ice Shelf drainage basin where slope reaches 0.3° over a 5-km length scale (Figure 2a, with LB outlined by the drainage basin between [lon,lat] of ~[45°E, 95°E,−70°N, −80°N]). The second region, we refer to as E-Ant, consists of all blocks outside LB where surface slopes are <0.1°. In E-Ant, *dh/dt* varies between −0.17 to 0.11 m/yr with mean and root-mean-square scatter (RMS) of −0.06 and 0.04 m/yr. Typical uncertainties of *dh/dt* range from ~0.01 m/yr in the interior to ~0.03 m/yr at the coast (Kalman filter covariance matrix estimate which depends on the assumed data noise, Figure 2b). In region LB, *dh/dt* varies between −0.13 to 0.21 m/yr with mean and RMS of 0.02 and 0.09 m/yr. The spatial distribution of *dh/dt* suggests a latitudinal dependency, with rates between −0.05 and 0.10 m/yr at latitudes [−70°, −73°] or [−86°, −81°], and between −0.15 and −0.05 m/yr at latitudes [−81°, −73°] (Figure 2a).

[7] To verify the results of *dh/dt* from the Kalman filter, profiles from repeated tracks are compared, and one example is shown in Figure 3. In this example, repeat tracks #1297 from Lasers 2a and 3a which are close to Lake Vostok ([−78.45°N, 106.87°E]) are shown before and after saturation correction. GLA06 heights are subtracted from the 5-km *a priori* DEM (Figure 3a) to obtain the first level of residuals (Figure 3b). Prior to saturation correction, heights from Laser 3a are lower than those from Laser 2a by −0.17 m. Received energies are ~25.1 ± 2.2fJ and 25.7 ± 1.4fJ for Lasers 3a and 2a, resulting in negative height biases of −0.26 ± 0.05 m and −0.28 ± 0.03 m. After the correction, heights in Laser 3a remain lower than those in Laser 2a by −0.15 m, resulting in a *dh/dt* of −0.15 m/yr for this single profile (the time separation is ~1 year between Lasers 2a and 3a). When all profiles within the block closest to Lake Vostok (block #221 [−78.5°N, 105°E]) are compared, height differences (Laser 3a minus 2a) are approximately −0.13 m and −0.06 m before and after saturation correction, and the Kalman filter estimate of *dh/dt* for the block is −0.06 m/yr.

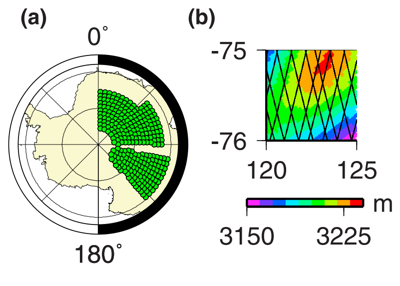

Figure 1. (a) The region of the grounded East Antarctic ice sheet used in this study and (b) an example of a (100km)^2 block. Within each block there are ~500 5-km DEM elements and 12–125 ICESat tracks (500–8000 data points).

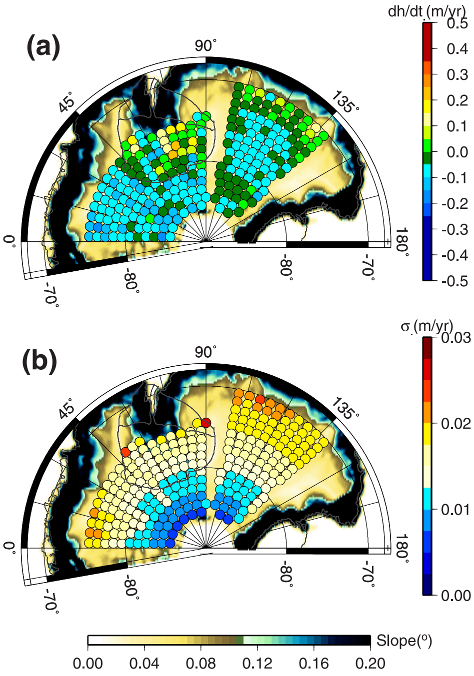

Figure 2. Results of (a) *dh*/*dt* and (b) uncertainties at the end of Laser 3a. The horizontal scale is surface slope, which is shown as the background field in the figure.

[8] To gain more insights into the *dh*/*dt* uncertainties, we evaluate *dh*/*dt* using ascending and descending tracks separately. For block #221 above, the mean and RMS of *dh*/*dt* are -0.01 ± 0.05 m/yr and -0.12 ± 0.08 m/yr for ascending and descending tracks respectively. The 40 cross-overs within this block have residuals (ascending minus descending) with mean and RMS of -0.05 ± 0.17 m and 0.13 ± 0.21 m for Laser 2a and 3a respectively. A crude estimate of *dh*/*dt* at the 40 cross-over locations yields a mean and RMS of -0.08 and 0.29 m/yr. Based on cross-over residuals, there are still clear biases between ascending and descending tracks in both laser periods. The shot-to-shot along track slope mean and RMS for this block is 0.02 and 0.06°. In general received energies are higher in Laser 3a than in 2a (~24.0fJ versus 22.3fJ for the block mentioned above), resulting in smaller height corrections for the latter. However, height differences (Laser 3a minus 2a) are consistently negative, approximately -0.10 to -0.04 m after corrections for the flattest part of E-Ant (Figure 2a). We suspect that pointing errors contribute to the negative *dh*/*dt* estimated here.

5. Error Assessment

[9] In our model we assumed that the model parameters are deterministic, i.e., no process noise, with initial variances of 400 m^2 for δ_{dem}, Δ_{DEM}, and 400 m^2/yr^2 for *dh*/*dt*. At the end of Laser 3a, the filter suggests uncertainties <0.03 m/yr for *dh*/*dt*. However, pointing bias produces systematic errors that are not accounted for in the filter. Current assessments of single-shot vertical accuracy are ~16 cm [*Schutz et al.*, 2005], and with pointing bias increase to ~21–33 cm for surface slope 0.1–0.5°. We assume a larger single-shot error of 1 m^2 as the first attempt to account for the pointing errors and coarseness in the parametrization of the surface.

[10] Towards the coast or near $-86°$ latitude, slopes become more systematic and pointing errors contribute pseudo *dh*/*dt* within the blocks. In addition, ICESat orbits with a ~0.33° tilt to avoid specular reflection, which results in a total pointing bias equivalent to that of 0.33° plus local slopes [*Schutz et al.*, 2005]. A sensitivity test between the time data were obtained (t ≈ [0.21, 0.79, 1.13, 1.38, 1.76] yr for Lasers 1–3a) and the model parameters shows that Laser 2c contributes the least to *dh*/*dt* estimates, and Lasers 2b–c contribute the most to the seasonal signal parameters. When only Lasers 2a and 3a are used, the contributions to the *dh*/*dt* estimate from both lasers are the same with opposite signs. Assuming negative height biases from columns 6–8 in Table 1, dh/dt_{bias} for Laser [2a, 3a] are ~[+0.02, -0.04]m/yr for 98% of the blocks with total slopes <0.4° in E-Ant, and [+0.03, -0.08]m/yr for region LB where total slope reaches 0.63°. If positive height biases are assumed, dh/dt_{bias} would have the same magnitudes but with signs reversed. In the worst case scenario, based on current pointing knowledge with Laser 3a having twice the height bias compared to Laser 2a, combined dh/dt_{bias} could

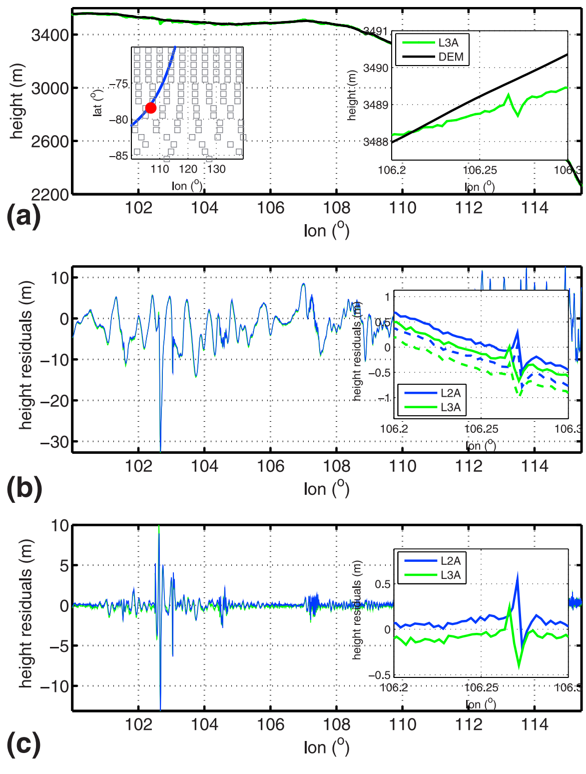

Figure 3. Height profiles for repeat tracks #1297 near Lake Vostok. (a) Profile of Laser 3a heights and the interpolated *a priori* DEM. The inset on the left shows the locations of the (100km)^2 blocks (gray), along with track #1297 (blue) and Lake Vostok location (red). (b) Height residuals (GLA06 heights minus DEM) for Lasers 2a and 3a. In the inset, dashed and solid lines are height residuals before and after saturation corrections, respectively. (c) Height residuals after two iterations using the Kalman filter.

reach ±0.06 m/yr over nearly flat terrains. In addition we only consider cases with one standard sigma of errors for pointing.

[11] In their analysis, *Luthcke et al.* [2005] showed that pointing errors can be both temporally and geographically correlated. *Fricker et al.* [2005] found over flat and smooth terrains, forward scattering and/or pointing errors give negative height biases of ~16 cm for Laser 2a. They also showed that, under clear sky conditions, pointing errors contribute negative height biases of about −1.9 and −1.2 cm for Laser 2a and 3a, and positive bias of 0.5 to 1.2 cm for Laser 2b. Between 82–91% of the data we use have gain = 13 for Laser 2a and 3a, and our data filtering scheme removes potential cloud (gain between 100 and 250). Thus pointing is the likely source of errors in our estimates of *dh/dt*.

6. Conclusion

[12] We have demonstrated the potential of ICESat data for surface change detection over Antarctica, using ICESat repeat track altimetry data and a combination of Kalman filtering and kriging. Currently only two laser operational periods (2a and 3a) have adequate pointing calibration to be used for height change detection. Results from the Kalman filter show over the smooth interior part of East Antarctica, *dh/dt* is negative with means between −0.10 to −0.05 m/yr. The mean error due to pointing biases is ~0.06 m/yr based on the data model/sensitivity. Due to a combination of lack of data and larger pointing errors than the science requirement of 2-arcsec, height change detection with an accuracy of ~0.02 m/yr is not possible at this time. However, the ICESat team anticipates the reduction of pointing errors in all laser operational periods to the same level as that in Laser 2a in the near future [*Schutz et al.*, 2005; *Luthcke et al.*, 2005]. When all available data, Lasers 1–3c become available with adequate pointing knowledge, our sensitivity test shows *dh/dt* uncertainties of 0.02 m/yr and 0.03 m/yr over surfaces with total slope of 0.33° (flat terrain) and 0.43° can be achieved. We are currently refining the technique to include parameters to account for pointing biases within each laser operational period, and will re-analyze using future data releases to improve *dh/dt* estimates and include the seasonal signal parameters.

[13] **Acknowledgments.** This research is supported by NASA Contract NAS5-99007. We thank NASA's ICESat Science Project and the NSIDC for distribution of the ICESat data, see http://icesat.gsfc.nasa.gov and http://nsidc.org/data/icesat. Thanks to D Yi, X Sun, H Fricker, S Luthcke, and B Schutz for the discussion on saturation correction and pointing errors, and special thanks to H Fricker, B Schutz and two anonymous reviewers for their helpful comments.

References

Brown, R. G., and P. Y. C. Hwang (1997), *Introduction to Random Signals and Applied Kalman Filtering*, 3rd ed., 484 pp., John Wiley, Hoboken, N. J.

Fricker, H. A., A. Borsa, B. Minster, C. Carabajal, K. Quinn, and B. Bills (2005), Assessment of ICESat performance at the salar de Uyuni, Bolivia, *Geophys. Res. Lett.*, *32*, L21S06, doi:10.1029/2005GL023423.

Luthcke, S. B., D. D. Rowlands, T. A. Williams, and M. Sirota (2005), Reduction of ICESat systematic geolocation errors and the impact on ice sheet elevation change detection, *Geophys. Res. Lett.*, *32*, L21S05, doi:10.1029/2005GL023689.

Olea, R. A. (1999), *Geostatistics for Engineers and Earth Scientists*, 303 pp., Springer, New York.

Schutz, B. E., H. J. Zwally, C. A. Shuman, D. Hancock, and J. P. DiMarzio (2005), Overview of the ICESat Mission, *Geophys. Res. Lett.*, *32*, L21S01, doi:10.1029/2005GL024009.

Zwally, H. J., A. C. Brenner, J. A. Major, R. A. Bindschadler, and J. G. Marsh (1989), Growth of Greenland Ice Sheet: Measurement, *Science*, *246*, 1587–1589.

Zwally, H. J., et al. (2002), ICESAT's laser measurements of polar ice, atmosphere, ocean, and land, *J. Geodyn*, *34*, 405–445.

A. T. Nguyen and T. A. Herring, Department of Earth, Atmospheric and Planetary Sciences, MIT, 77 Massachusetts Avenue, Building 54-616, Cambridge, MA 02139, USA. (atnguyen@chandler.mit.edu)